Journal of Molecular Liquids 319 (2020) 114302

Contents lists available at ScienceDirect

Journal of Molecular Liquids

journal homepage: www.elsevier.com/locate/molliq

Green fabrication of reduced graphene oxide decorated with Ag nanoparticles (rGO/Ag NPs) nanocomposite: A reusable catalyst for the degradation of environmental pollutants in aqueous medium

Saba Hemmati [a], Majid M. Heravi [a,*], Bikash Karmakar [b], Hojat Veisi [c,*]

[a] Department of Chemistry, School of Science, Alzahra University, PO Box 1993891176, Vanak, Tehran, Iran
[b] Department of Chemistry, Gobardanga Hindu College, India
[c] Department of Chemistry, Payame Noor University, Tehran, Iran

ARTICLE INFO

Article history:
Received 6 August 2020
Received in revised form 5 September 2020
Accepted 9 September 2020
Available online 11 September 2020

Keywords:
Silver
Graphene oxide
Nanocatalyst
Reduction
Waste-water treatment

ABSTRACT

In this current work, a bio-inspired green approach has been followed to synthesize Ag nanoparticles (NPs), which were immobilized over reduced graphene oxide (rGO) as a suitable support. In the stepwise preparation of the bionanocomposite (rGO/Ag NPs) by using *Menthapulegium* flower extract, initially graphene oxide (GO) was reduced to rGO followed by in situ reduction of Ag^{+} ions to Ag NPs. In these reductions, different biomolecules such as, polyphenols, flavonoids, alkaloids, terpenoids and mild acids were employed as the natural reductant. The oxygenated functions in the aforementioned biomolecules, efficiently, assisted the capping and stabilizing the AgNPs. The as-synthesized nanocomposite was fully characterized using different techniques such as, UV–Vis spectroscopy, scanning electron microscopy (SEM), energy-dispersive X-ray spectroscopy (EDX), wavelength dispersive X-ray spectroscopy (WDX) elemental mapping, transmission electron microscopy (TEM), X-ray diffraction (XRD) and inductively coupled plasma (ICP). Diameter of the biosynthesized Ag NPs were found to be in the range of 20–25 nm. The constituent elements were found to be homogeneously dispersed as found from elemental mapping study. This novel prepared nano-composite showed excellent water dispersibility due to the hydrophilicity of biomolecules attached to them, which is essential criterion in heterogeneous catalysis. This composite was used as an effective catalyst in the reductive degradation of water contaminated by organic dyes such as methyl Orange (MO) and rhodamin B (RhB) using $NaBH_4$ as reductive agent at room temperature. The progress of reduction was monitored by UV–Vis spectroscopy. Both the reactions followed pseudo-unimolecular kinetics and the corresponding rate constants were found being 0.098 s^{-1} and 0.096 s^{-1} respectively. The material was significantly robust as justified by the leaching as well as hot-filtration tests and its reusability for several times without any appreciable loss in its activity.

1. Introduction

In the last few decades nanotechnology has been considered as one of the most emerging field in science. This technology has appeared extremely promising, due to its extensive applications in different arena like physics, chemistry, biology, engineering and their interdisciplinary regions [1–3]. Nanosciences have been exploited in different fields like applicative pharmacology, drug delivery targeting cancer cell and other deadly ailments [4], disposal of heavy and toxic metals, degradation of environmental contaminants, water purifications [5], electronics [6], imaging contrast agents [7] sensor and catalysis [8–11]. Scientist are particularly interested in nanocatalysis, based on the unique criteria of the materials, like NPs have extremely small dimension, high surface to volume ratio, exceptional shape dependant properties, uniformity in particle size distribution, truly heterogeneous nature and reusability with almost constant efficiency [12–15]. They satisfy almost all the criteria as for an ideal catalyst. Green chemistry offers a cohesive set of twelve principles and has engrossed widespread interest in view of sustainability [16]. One of the most important future perspectives of green chemistry is designing ecological or bio-inspired catalysts in pursuing important organic transformations. The

* Corresponding authors.
E-mail addresses: mmheravi@alzahra.ac.ir (M.M. Heravi), hojatveisi@yahoo.com (H. Veisi).

https://doi.org/10.1016/j.molliq.2020.114302
0167-7322/

concept of greener nanoscience is a practical application of advanced nanotechnology [17–20]. Following this coalescence between nanotechnology and green chemistry, the biogenic synthesis of NPs has evolved as an outstanding approach in the design of eco-friendly catalysts.

Extract of different parts of plants like fruits, barks, flowers, roots leaves contain several phytochemicals like polyphenols, flavonoids, alkaloids, terpenoids and mild acids which have been found to be very effective in the biometric conversion of metal salts into corresponding NPs [21–26]. In the recent past, this green metric protocol for the synthesis of noble metal NPs has been quite popular [27–30]. Among the different noble metals Ag NPs are relatively less expensive as compared to Au, Pd and Pt. They also find extensive applications in diverse fields like biological transmission electron microscopy, colorimetric DNA sensor, animal husbandry, agriculture, household, packaging, optics, electronics and catalysis [31,32]. Thereby, ample studies are going on for the biogenic synthesis of Ag NPs [33–38]. Nevertheless, due to ultrafine size, large specific surface area and strong electrostatic attraction, the NPs are frequently found to form nano-clusters by self-aggregation which considerably reduces their catalytic efficiency. This can be restricted by homogeneous immobilization of the NPs over a suitable support [39–41].

Among various suitable materials as support, graphene and its derivatives have gained utmost importance due to their high thermal and mechanical stability, exceptional electrical conductivity with incredibly large surface area and adsorption ability. These unique materials are endowed with atomic width and a densely packed two-dimensional honeycomb like structures [42].

In continuation to our current venture on the design and synthesis of sustainable catalytic nanomaterials [39–50], we have synthesized Ag NPs following biogenic technique and incorporated them over the surface of bioreduced graphene oxide (rGO/Ag NPs). For the green reduction of GO and Ag^+ ions we exploited the *Menthapulegium* flower extract, a rich source in polyphenols, terpenoids, alkaloids and polysaccharide moieties. The plant has high ornamental and medicinal values being used as anti-hypertensive, antitussive and expectorant in traditional medicine [51,52].

The increasing social development has upgraded the human lifestyle but at the cost of environmental pollution. The lack in consciousness and inadequate control measures has caused serious damage to the ecological parameters. Contamination of harsh chemicals, heavy metals, drugs and pharmaceuticals, hormones and dyes into wastewater effluent and thereafter into natural waters has been a major issue. A bulk amount of synthetic dyes is released into water by textile, dye, paint, print and paper industries as a result of incomplete quenching of pigments and successive washing of colored materials [53]. Even at a minute concentration the dyes are highly diffusible into water which obstructs the penetration of sunlight. This, in turn, decreases the dissolution of oxygen into water, causes death of photosynthetic organisms which ultimately leads to disruption of aquatic ecosystem. Hence, the wastewater treatment by disposal of these organic dyes following suitable techniques is of great importance, in view of sustainable management [54–56]. In this regard, catalytic reduction of dyestuffs involving nanomaterials nowadays, is considered as one of the promising, cost-effective and energy efficient green methods, [41,57–62]. This strategy successfully transforms the organic pollutants to safer chemicals being tender to natural waters.

Consequently, in this current study we wish to report the catalytic degradation of two harmful organic dyes, Methyl orange (MO) and Rhodamine B (RhB), using novel composite, bionanocomposite (rGO/Ag NPs). The reduction was carried out using $NaBH_4$ at aqueous media and was completely monitored over time dependant UV–Vis spectroscopy. Both the reactions were completed within 50 s with almost quantitative yield. Subsequently, using the UV data, kinetics of the reactions was also studied. In addition, the catalyst was easily isolated from the reaction mixture by centrifugation and reused several times without significant decrease in catalytic activity. Robustness of the material was further investigated using hot filtration and leaching test.

2. Experimental

2.1. Preparation of Menthapulegium flower extract

Fresh *Menthapulegium* flowers were collected and washed thoroughly with double-distilled water. 2.0 g of the flower petals were extracted in 100 mL deionized water by boiling for 20 min. The colored solution was then cooled and filtered through Whatmann-1 filter paper. It was stored at 4 °C in refrigerator for further use.

2.2. Biogenic synthesis of rGO/Ag NPs nanocomposite using Menthapulegium flower extract

GO was prepared following a procedure modified by Hummers et al. [63]. 100 mg of GO was dispersed in the *Menthapulegium* flower extract by sonication for 20 min followed by refluxing for 2 h. Complete reduction of GO was confirmed by change in color of the solution from light brown to black due to excitation of surface Plasmon resonance. The rGO was isolated by centrifugation followed by washing with DI water. In the next step, the rGO was dispersed again in the flower extract by sonication and 10 mL aqueous solution of $AgNO_3$ (0.05 g/L) was added dropwise. The mixture was then agitated at 100 °C for 30 min. Finally, the rGO/Ag NPs nanocomposite was retrieved from the reaction mixture in a centrifuge, rinsed thoroughly with DI water and subsequently dried in air. ICP-OES technique was used to quantify the Ag load on the composite, which was found to be 0.096 mmol/g.

2.3. Reductions of MO and RhB: general procedure

In a 25 mL aqueous solution of MO or RhB (0.0002 M), 0.003 g of the rGO/Ag NPs nanocomposite was shaken at room temperature for 1 min. Fresh $NaBH_4$ solution (25 mL, 0.2 M) was then added to the mixture and stirred till the colored solution became colorless. The progress of reaction was monitored using UV–Vis spectroscopy. After completion of the reaction, the catalyst was separated from reaction mixture by centrifugation, washed with H_2O/EtOH and recovered being used in next runs.

3. Results and discussion

3.1. Characterization of catalyst by its data analysis

The rGO/Ag NPs nanocomposite was synthesized biogenically in stepwise fashion. The oxygenated functions including the polyhydroxy organic groups present in Menthapulegium flower extract first competently reduces the GO to rGO under ultrasonic conditions. The electron rich oxygen functions thereafter transfers their electrons to the surface anchored Ag^+ ions to reduce it to Ag NPs in situ. The tiny NPs also gets capped and stabilized by the biomolecules of flower extract (Scheme 1). The as synthesized nanocomposite was characterized with UV–Vis, SEM, EDX, atomic mapping, TEM, powder XRD and ICP-OES techniques.

Fig. 1 represents the overlapping UV spectra of GO and rGO/Ag NPs. GO exhibits a characteristic absorption maxima at 235 nm attributed to the $\pi \rightarrow \pi^*$ transitions of C—C bonds from aromatic moiety and a shoulder at 280 nm due to the $n \rightarrow \pi^*$ transition of C═O function. In its reduction to rGO, the visible change from is observed from light to dark brown solution, due to reduction of hydrophilic functional groups like carboxyl, hydroxyl and epoxide. Spectroscopically, this change is displayed from a bathochromic shift from

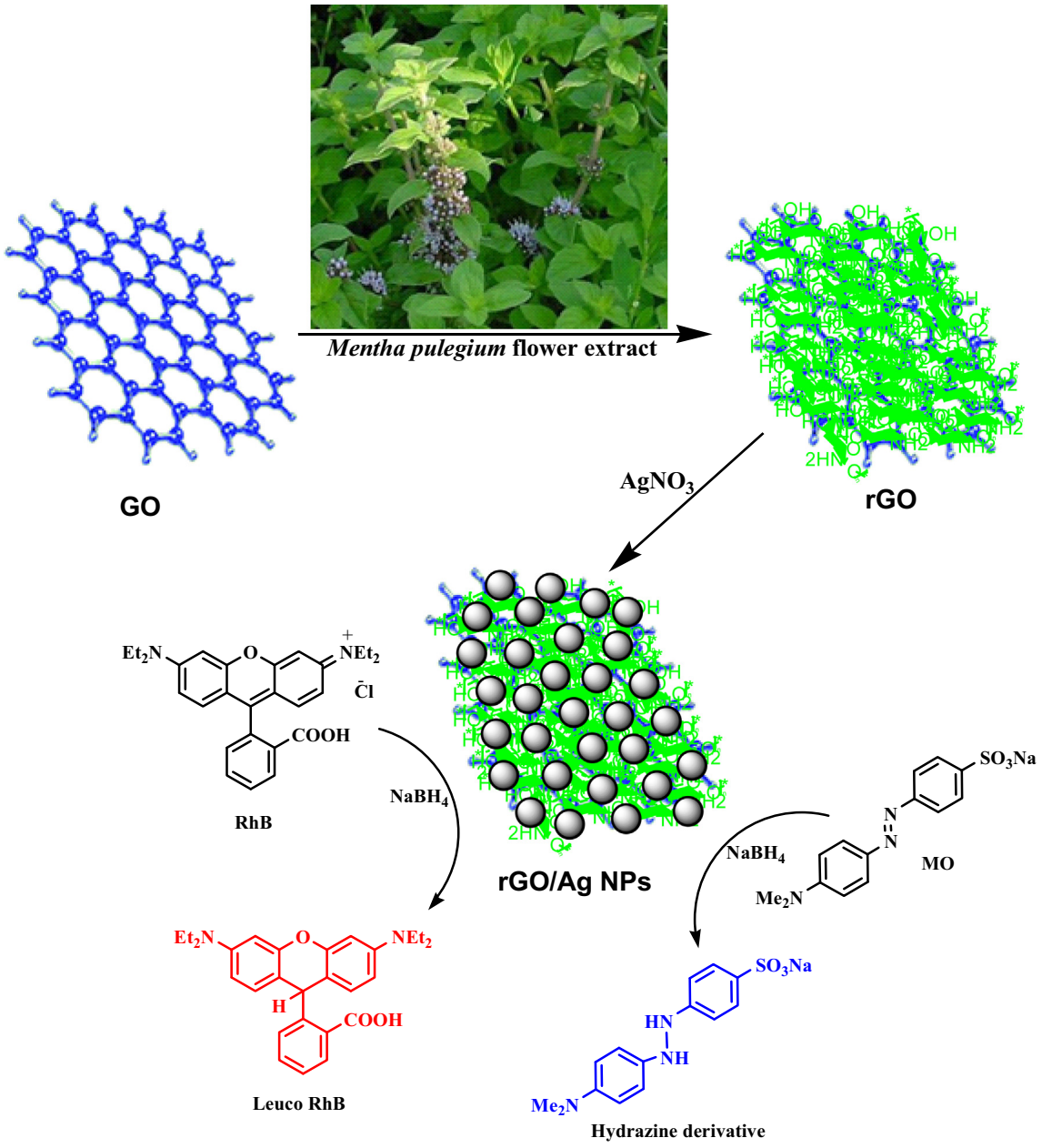

Scheme 1. Fabrication of rGO/Ag NPs nanocomposite using *Menthapulegium* flower extract and its catalytic application in the reduction of MO and RhB.

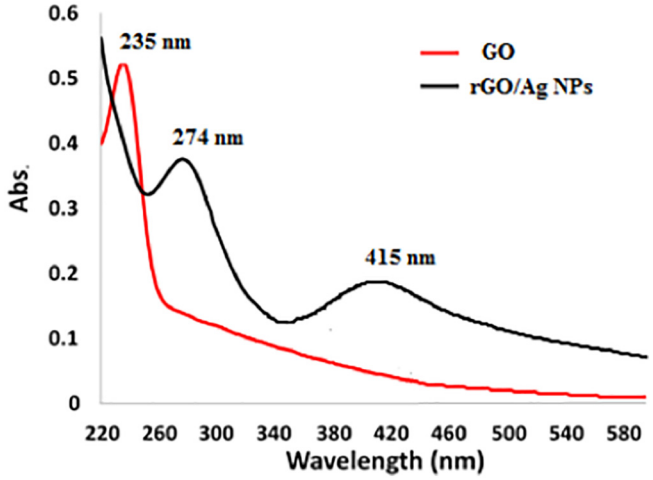

Fig. 1. UV–Vis spectra of GO and the biosynthesized rGO/Ag NPs nanocomposite.

~235 nm peak (GO) to ~274 nm (rGO). Fig. 1 clearly depicts the difference. [42]. The electronic conjugation within graphene sheet is restored upon green reduction, reflecting increased π-electron density and structural rearrangements. The appearance of a new peak at 415 nm is corroborated to the Ag NPs being formed from Ag ions. However, the biomolecules being attached to the material could not be identified from UV–Vis spectra.

The morphological appearance and microstructures of the pre-prepared rGO/Ag NPs nanocomposite was investigated by SEM which is displayed in Fig. 2. The GO image represents a thin transparent sheet with wrinkled morphology throughout. It looks like a turned cloth, edges of which are seen to be partly folded (Fig. 2a). In the SEM image of rGO/Ag NPs nanocomposite the white spherical balls representing the Ag NPs are seen to be evenly distributed on the shrink surface of rGO (Fig. 2b). On close observation, a thin layer of the biomolecules can be seen over the Ag NPs. An EDX analysis of the nanocomposite documents its exact chemical compositions. Fig. 3 represents the EDX profile with Ag, C and O as the main

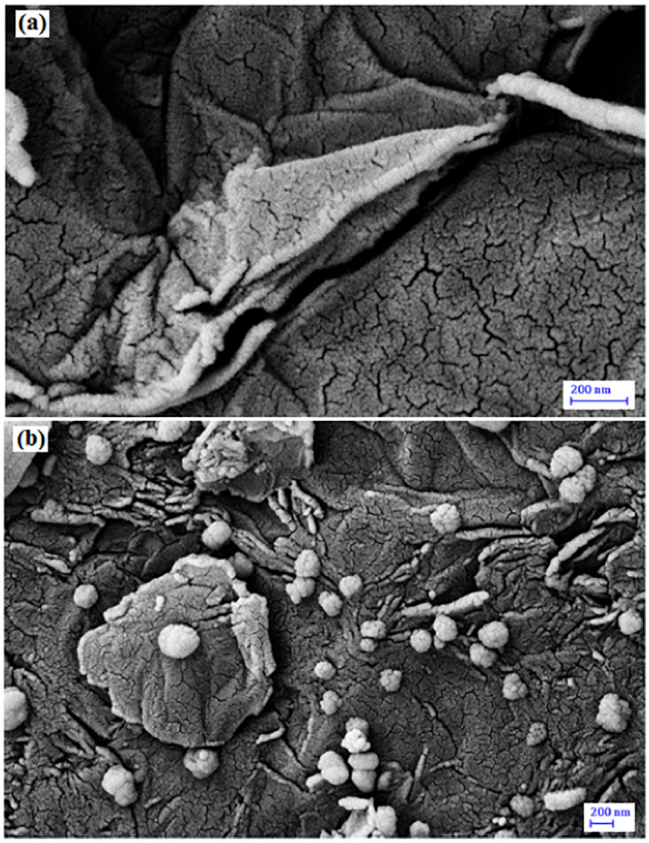

Fig. 2. SEM images of (a) GO and (b) the rGO/Ag NPs nanocomposite.

constituent of the material. The presence of C and O could be justified for the polyphenolic attachments.

The EDX data was further validated with WDX atomic mapping image. It displays a clear picture of atomic distributions over the material surface. An X-ray scan of the SEM image segment is used in the WDX mapping analysis, as shown in Fig. 4. The C, O and Ag atoms are observed to be uniformly distributed over the surface. In some regions the Ag atoms seem to form clusters. The EDX and

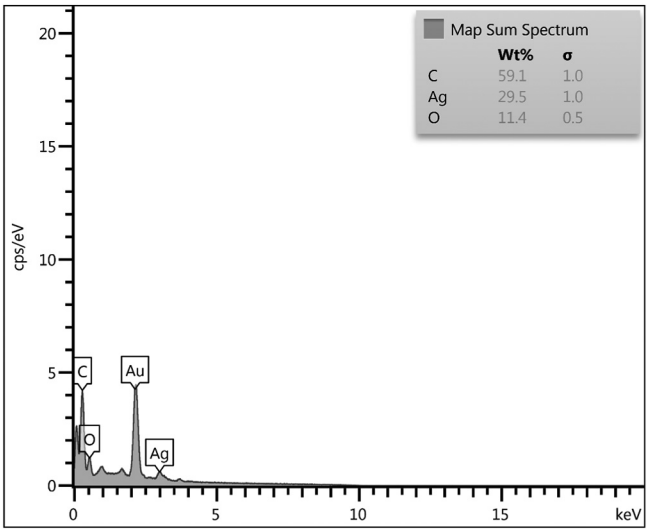

Fig. 3. EDX spectrum of the rGO/Ag NPs nanocomposite.

WDX data in turn also justifies the successful formation of the nanocomposite.

To get a deeper insight of the structural morphology of rGO/Ag NPs nanocomposite, TEM analysis was carried out. As can be seen from Fig. 5, the black dots spread homogeneously over the transparent rGO sheet, symbolizes the Ag NPs. Mean diameter of Ag NPs were around ~15–25 nm.

Crystallinity and phase structure of the rGO/Ag NPs nanocomposite was investigated over XRD analysis. Fig. 6 illustrates the single phase diffractogram of the material which signifies that Ag NPs are perfectly embedded over rGO and behaves as a single entity. It represents the four significant sharp diffraction peaks at $2\theta = 38.1°$, 44.3°, 64.4°, 77.4°, attributed to diffraction over (1 1 1), (2 0 0), (2 2 0) and (3 1 1) planes of cubic Ag crystalline phases (JCPDS No. 04-0783). The broad region at $2\theta = 10–25°$ (002) corresponds to the amorphous rGO moiety.

3.2. Catalytic reduction of MO and RhB over rGO/Ag NPs nanocomposite

After full characterization of the synthesized nanocomposite, its catalytic performance was examined. Reduction of two water contaminated organic dyes, viz., MO and RhB in presence of $NaBH_4$ as reducing agent in the presence of rGO/Ag NPs nanocomposite was investigated. Progress of the reaction was fully monitored using a UV–Vis spectrophotometer. Dilute aqueous solution of the dye assumed a specific color prior to the addition of borohydride and catalyst. As the reaction started, color of the solution started fading within seconds, an indication of the degradation. This change in color is associated with the change in absorption frequency (λ_{max}) recorded by the UV–Vis spectrophotometer. Fig. 7a displays the time dependent absorbance plots of the reduction of MO in presence of 0.003 g of rGO/Ag NPs nanocomposite. As shown in the plot, the initial absorption maxima at 465 nm gradually diminishes with time and after a time lapse of 50s, the bell shaped plot became flattened. This also visibly could be seen from the colorless reaction mixture. Next, we studied the reaction kinetics for the reduction of the two dyes over $NaBH_4$. As the concentration of $NaBH_4$ remained constant throughout the reaction, it can be assumed that the reaction followed a pseudo-first-order kinetics. Accordingly, it follows the Lambert-Beer's equation $\ln(A_t/A_0) = kt$, where A_0 is the initial absorbance and A_t is the absorbance at time t in second. From the slope of the plot of $\ln(A_t/A_0)$ vs t, the rate constant for the catalytic reduction of MO using 0.003 g of catalyst was found to be 0.098 s^{-1} (Fig. 7b). The similar trend was followed in the reduction of RhB (λ_{max} 550 nm) affording excellent results in short reaction time (50s). The results have been displayed in Fig. 8a. In this case the rate constant was found to be 0.096 s^{-1} and the corresponding plot has been presented in Fig. 8b.

While concerning about green and sustainable chemistry, reusability of the catalyst is an obvious measure. In this regard, after completion of a fresh batch of probe reactions, the catalyst was recovered by centrifugation and washed with EtOH:H_2O (1:1). It was then dried and reused in further batches applying the same conditions. The results revealed that rGO/Ag NPs nanocomposite retained its activity up to 10 successive runs without significant loss in its catalytic activity in the reduction of MO and RhB (Fig. 7c and c).

In order to ascertain the robustness of our catalyst, the Ag leaching was inspected with the 10 time used catalyst. Gratifyingly, the leaching was insignificant in both reductions (0.01 wt% of the initial load). Furthermore, the true heterogeneity nature of the rGO/Ag NPs nanocomposite was assessed through a hot filtration test in the reduction of MO under already secured optimal conditions. The reaction was stopped after 25 s when about 60% yield was obtained and the catalyst was isolated from the reaction mixture. Then the catalyst-free hot filtrate was further stirred for

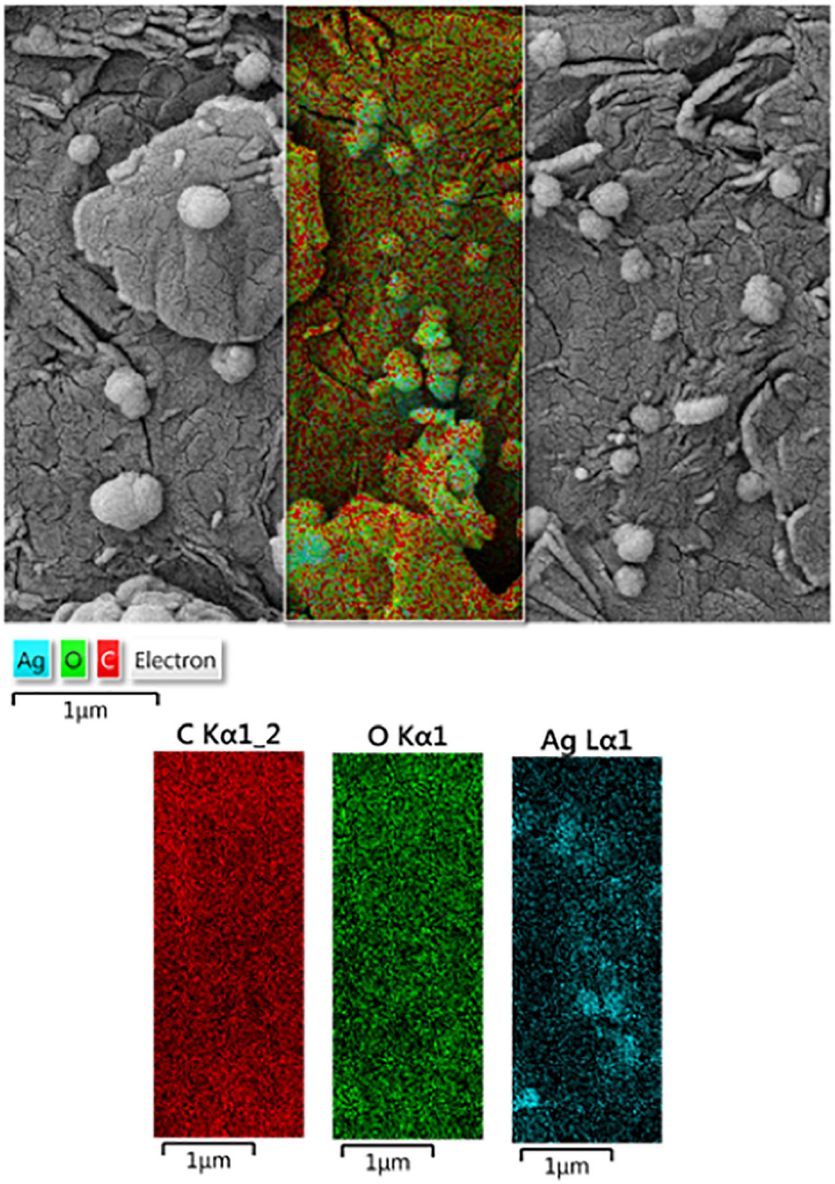

Fig. 4. WDX atomic mapping of the rGO/Ag NPs nanocomposite.

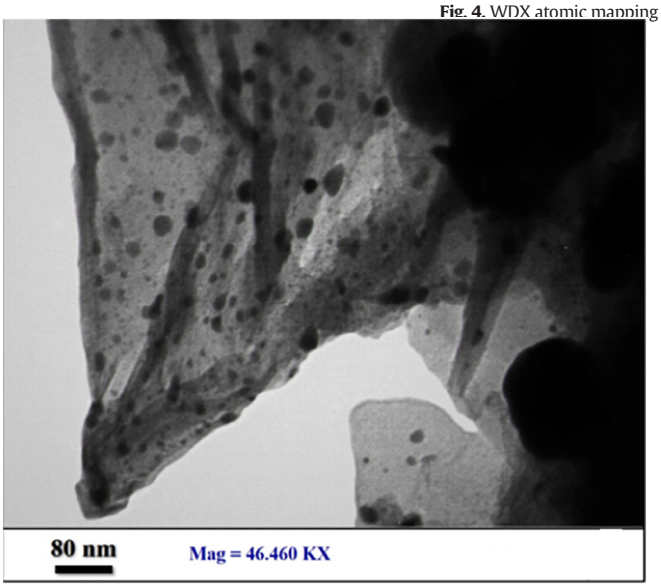

Fig. 5. TEM image of the rGO/Ag NPs nanocomposite.

another 25 s. Incidentally, the reaction hardly proceeded within this period (Fig. 7d). This was also an indication for the insignificant leaching of Ag species into the reaction mixture. In fact, ICP-OES analysis of the filtrate justified that there was no leaching of

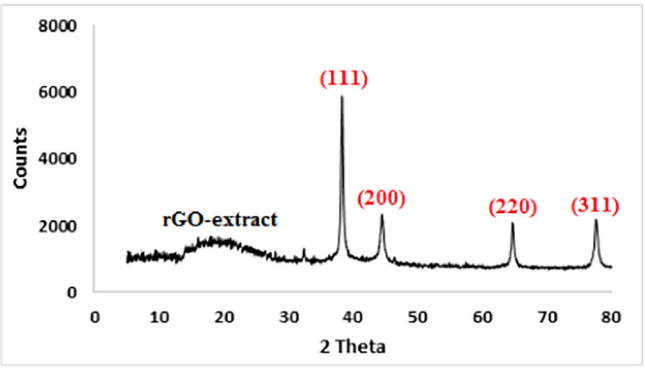

Fig. 6. XRD pattern of the rGO/Ag NPs nanocomposite.

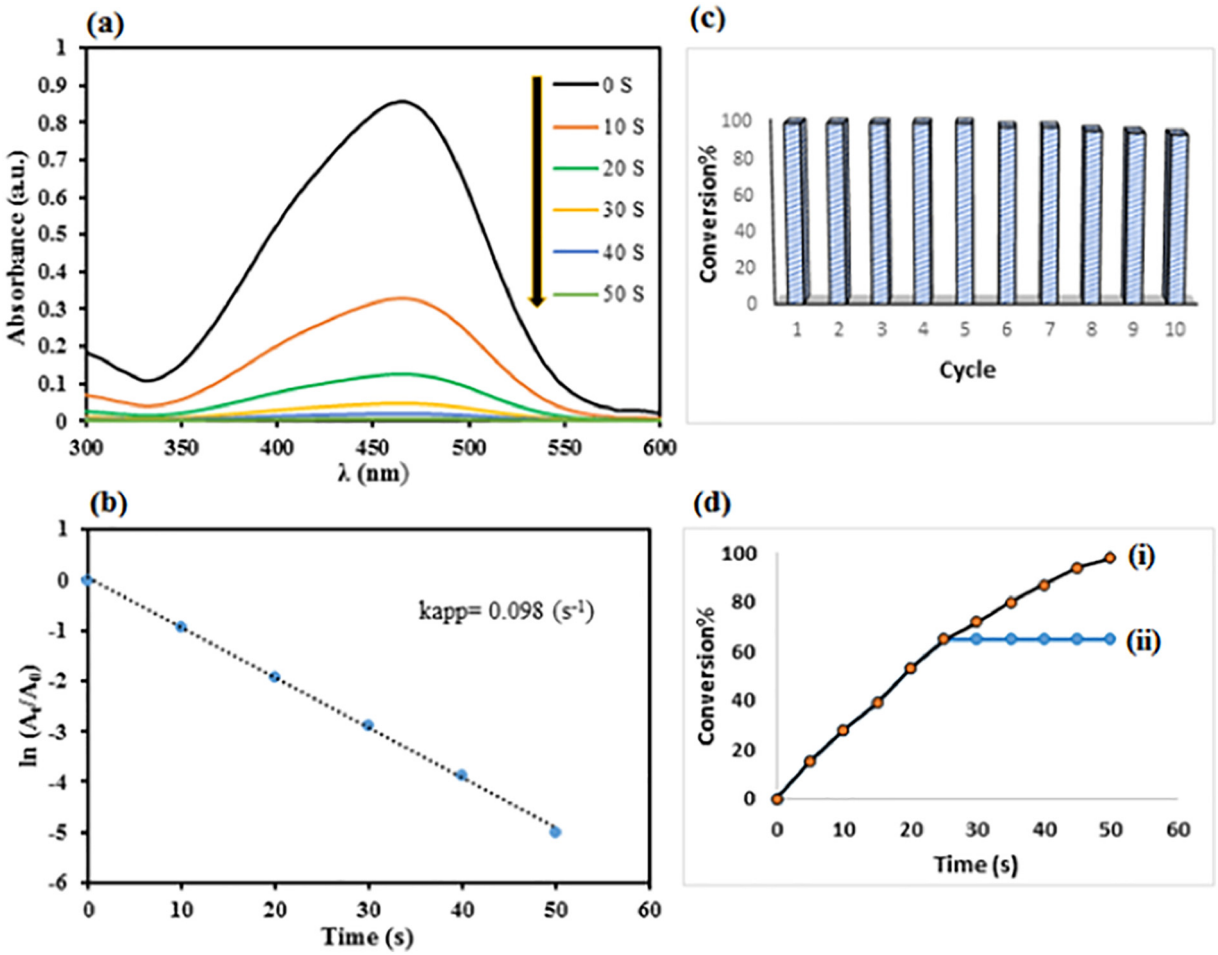

Fig. 7. (a) The absorption profile in the reduction of MO catalyzed over rGO/Ag NPs nanocomposite, (b) Its kinetic plots ($\ln A_t/A_0$ vs t), (c) reusability of rGO/Ag NPs nanocomposite for the reduction of MO, and (d) Product yield vs time (i; with catalyst) and the hot filtration run (ii, without catalyst).

Ag species into the reaction solution, which confirms the true heterogeneous nature of the composite. The same experiment was conducted with RhB reduction and similar results were obtained (Fig. 8d).

3.3. The mechanistic study

A reasonable mechanistic pathway for the reduction of MO and RhB dyes over rGO/Ag NPs nanocomposite in aqueous medium has been suggested as depicted in Scheme 2. $NaBH_4$ initially dissociates to produce borohydride ions which get adsorbed over the surface of Ag NPs. In the meantime, the dye is also adsorbed over the catalyst surface via π-π stacking interactions. H^- ions are then transferred to the dye and it is reduced. Eventually, the reduced dye leaves the nanocomposite surface making the catalytic site free for the next cycle [64].

In order to display the significant benefit of the mentioned approach in this study, compared to literature, some of results for MO reduction are listed in Table 1. The results show that the rGO/Ag NPs nanocomposite is an efficient catalyst considering the rate constant comparing with the before reported catalysts.

4. Conclusion

In summary, we have introduced a water dispersible rGO/Ag NPs nanocomposite following a biogenic green approach using *Menthapulegium* flower extract. Tiny Ag NPs were homogeneously dispersed and anchored over reduced GO surface exploiting the herb bio-ingredients. They also help to cap and stabilize the NPs. The protocol involves mild and clean reaction conditions and devoid of harsh chemicals and solvents. We demonstrated that rGO/Ag NPs nanocomposite could efficiently catalyze the reduction of MO and RhB dyes in short reaction times, in the presence of the $NaBH_4$ as reductant, being followed up over UV–Vis spectrophotometer. The excellent recyclability, minute leaching and true heterogeneity confirmed the high robustness of our prepared nanocomposite.

CRediT authorship contribution statement

I have to add that this submission is original and all co-authors are contributed and aware of the submission and also agree to its publication in the *J Mol Liquid*. This work is novel/original and is not under consideration for publication elsewhere.

Seba Hemmati: Investigation, Formal analysis. **Majid Heravi**: Supervision, Investigation, Validation. **Bikash Karmakar**: Writing - review & editing, Formal analysis. **Hojat Veisi**: Planning, Writing - original draft.

Declaration of competing interest

The authors declare that they have no known competing financial interests or personal relationships that could have appeared to influence the work reported in this paper.

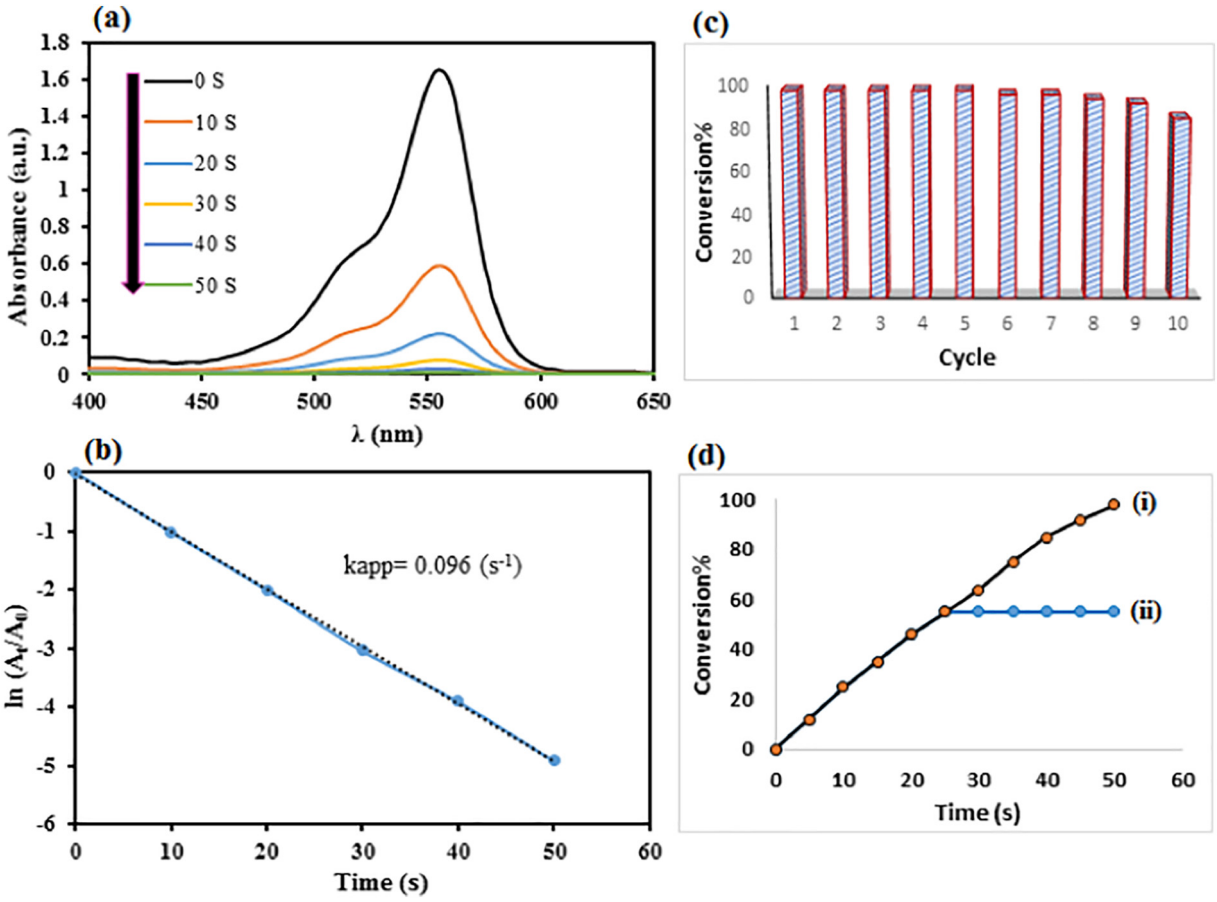

Fig. 8. (a) The absorption profile in the reduction of RhB catalyzed over rGO/Ag NPs nanocomposite, (b) Its kinetic plots (ln A_t/A_0 vs t), (c) reusability of rGO/Ag NPs nanocomposite for the reduction of RhB, and (d) Product yield vs time (i; with catalyst) and the hot filtration run (ii, without catalyst).

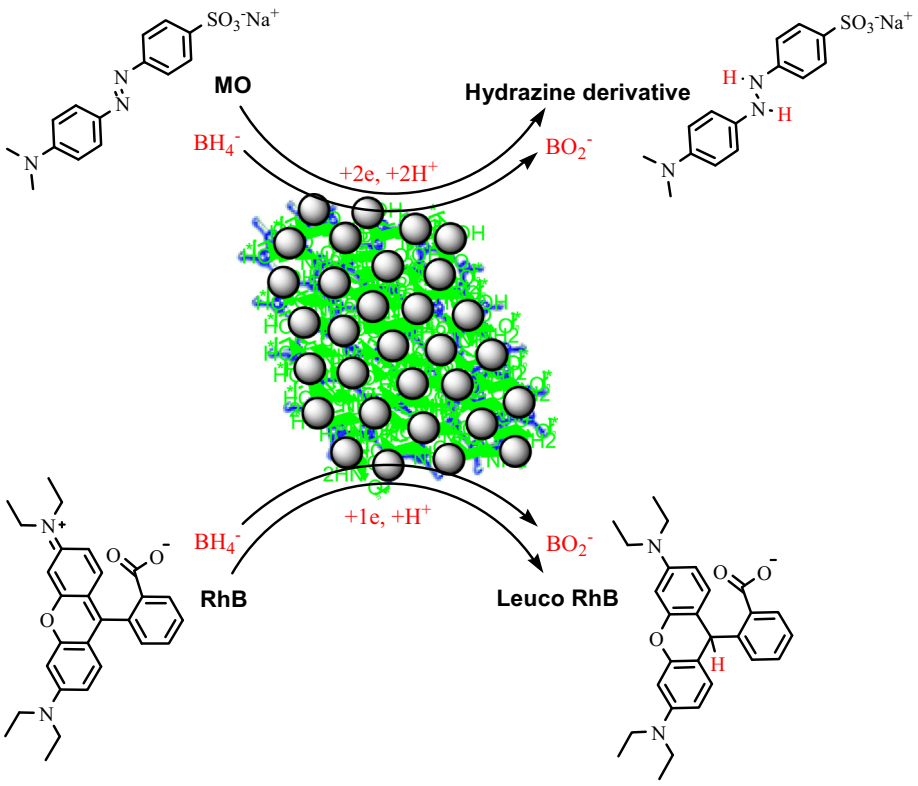

Scheme 2. Mechanism for the reduction of MO and RhB by rGO/Ag NPs nanocomposite.

Table 1
Comparison of the catalytic capacities of various catalysts reported in the literature for the reduction of MO by $NaBH_4$.

Entry	Catalyst	T (K)	k (s^{-1}) × 10^{-3}	Ref.
1	Fe_3O_4-g-C_3N_4-TCT-PAA-Ag	298	45	[31]
2	Ag-γ-Fe_2O_3@CS	298	61	[65]
3	TiO_2	303	52	[66]
4	Fe_3O_4/Hal-Mel-TEA(IL)-Pd	293	45	[61]
5	CuO nanostructure	308	11	[67]
6	Co:La:TiO_2	303	77	[66]
7	SGCN/Fe_3O_4/PVIs/Pd	298	52	[68]
8	SGCN/Fe_3O_4/PVIs/Pd	303	115	[68]
9	rGO/Ag NPs nanocomposite	298	98	This work

Acknowledgments

SH and MMH are thankful Alzahra University Research Council and Elites Federation. HV is grateful to Payame Noor University (PNU) for financial supports and BK thanks Gobardanga Hindu College for affiliation.

References

[1] L. Liu, A. Corma, Metal catalysts for heterogeneous catalysis: from single atoms to nanoclusters and nanoparticles, Chem. Rev. 118 (2018) 4981–5079.
[2] R.J. Hamers, Nanomaterials and global sustainability, Acc. Chem. Res. 50 (2017) 633–637.
[3] J.E. Hutchison, The road to sustainable nanotechnology: challenges, progress and opportunities, ACS Sustain. Chem. Eng. 4 (11) (2016) 5907–5914.
[4] P. Gao, W. Pan, N. Li, B. Tang, Boosting cancer therapy with organelle-targeted nanomaterials, ACS Appl. Mater. Interfaces 11 (2019) 26529–26558.
[5] M. Wang, S.K. Mohanty, S. Mahendra, Nanomaterial-supported enzymes for water purification and monitoring in point-of-use water supply systems, Acc. Chem. Res. 52 (3) (2019) 876–885.
[6] D. Son, Z. Bao, Nanomaterials in skin-inspired electronics: toward soft and robust skin-like electronic nanosystems, ACS Nano 12 (2018) 11731–11739.
[7] N. Naseri, E. Ajorlou, F. Asghari, Y. P-Soltanahmadi, An update on nanoparticle-based contrast agents in medical imaging, Artif. Cells, Nanomed., Biotechnol. 46 (2018) 1111–1121.
[8] Q. Zhang, X. Yang, J. Guan, Applications of magnetic nanomaterials in heterogeneous catalysis, ACS Appl. Nano Mater. 2 (2019) 4681–4697.
[9] M. Hu, Z. Yao, X. Wang, Graphene-based nanomaterials for catalysis, Ind. Eng. Chem. Res. 56 (2017) 3477–3502.
[10] N. Sharma, H. Ojha, A. Bharadwaj, D.P. Pathak, R.K. Sharma, Preparation and catalytic applications of nanomaterials: a review, RSC Adv. 5 (2015) 53381–53403.
[11] K. Shen, X. Chen, J. Chen, Y. Li, Development of MOF-derived carbon-based nanomaterials for efficient catalysis, ACS Catal. 6 (2016) 5887–5903.
[12] C.A. Antonyraj, J. Jeong, B. Kim, S. Shin, S. Kim, K.Y. Lee, J.K. Cho, Selective oxidation of HMF to DFF using Ru/γ-alumina catalyst in moderate boiling solvents toward industrial production, J. Ind. Eng. Chem. 19 (3) (2013) 1056–1059.
[13] S. Menon, S. Rajeshkumar, S. Venkatkumar, A review on biogenic synthesis of gold nanoparticles, characterization, and its applications, Resource-Efficient Technologies 3 (2017) 516–527.
[14] M. Yazdankhah, H. Veisi, S. Hemmati, *In situ* immobilized palladium nanoparticles (Pd NPs) on *fritillaria imperialis* flower extract-modified graphene and their catalytic activity for reduction of 4-nitrophenol, J. Taiwan Inst. Chem. Eng. 91 (2018) 38–46.
[15] Y. Xia, H. Yang, C.T. Campbell, Nanoparticles for catalysis, Acc. Chem. Res. 46 (8) (2013) 1671–1672.
[16] P. Anastas, N. Eghbali, Green chemistry: principles and practice, Chem. Soc. Rev. 39 (2010) 301–312.
[17] P. Anastas, M.M. Kirchhoff, Origins, current status, and future challenges of green chemistry, Acc. Chem. Res. 35 (2002) 686–694.
[18] J.H. Clark, Solid acids for green chemistry, Acc. Chem. Res. 35 (2002) 791–797.
[19] J.E. Hutchison, Greener nanoscience: a proactive approach to advancing applications and reducing implications of nanotechnology, ACS Nano 2 (2008) 395–402.
[20] R.S. Varma, Journey on Greener Pathways: From the Use of Alternate Energy Inputs and Benign Reaction Media to Sustainable Applications of Nano-Catalysts in Synthesis and Environmental Remediation, 16, 2014 2027–2041.
[21] R. Mohammadinejad, S. Karimi, S. Iravani, R.S. Varma, Plant-derived nanostructures: types and applications, Green Chem. 18 (2016) 20–52.
[22] S. Machado, S.L. Pinto, J.P. Grosso, H.P.A. Nouws, J.T. Albergaria, C. Delerue-Matos, Green production of zero-valent iron nanoparticles using tree leaf extracts, Sci. Total Environ. 445 (2013) 1–8.
[23] G. Lopez-Tellez, P. Balderas-Hernandez, C.E. Barrera-Diaz, A.R. Vilchis-Nestor, G. Roa-Morales, B. Bilyeu, Green method to form iron oxide nanorods in orange peels for chromium (VI) reduction, J. Nanosci. Nanotechnol. 13 (2013) 2354–2361.
[24] K.M. Kumar, B.K. Mandal, K.S. Kumar, P.S. Reddy, B. Sreedhar, Biobased green method to synthesise palladium and iron nanoparticles using Terminalia chebula aqueous extract, Spectrochim. Acta A 102 (2013) 128–133.
[25] O.V. Kharissova, H.V.R. Dias, B.I. Kharisov, B.O. Pérez, V.M. Pérez, The greener synthesis of nanoparticles, Trends in Biotechnol. 31 (2013) 240–248.
[26] D. Sharma, S. Kanchi, K. Bisetty, Biogenic synthesis of nanoparticles: a review, Arab. J. Chem. 12 (2019) 3576–3600.
[27] M.N. Nadagouda, N. Iyanna, J. Lalley, C. Han, D.D. Dionysiou, R.S. Varma, Synthesis of silver and gold nanoparticles using antioxidants from blackberry, blueberry, pomegranate, and turmeric extracts, ACS Sustain. Chem. Eng. 2 (2014) 1717–1723.
[28] M. Sarmah, A.B. Neog, P.K. Boruah, M.R. Das, P. Bharali, U. Bora, Effect of substrates on catalytic activity of biogenic palladium nanoparticles in C–C cross-coupling reactions, ACS Omega 4 (2019) 3329–5340.
[29] P. Vishnukumar, S. Vivekanandhan, S. Muthuramkumar, Plant-mediated biogenic synthesis of palladium nanoparticles: recent trends and emerging opportunities, ChemBioEng. Rev. 4 (2017) 18–36.
[30] D. Sun, G. Zhang, X. Jiang, J. Huang, X. Jing, Y. Zheng, J. He, Q. Li, Biogenic flower-shaped Au–Pd nanoparticles: synthesis, SERS detection and catalysis towards benzyl alcohol oxidation, J. Mater. Chem. A 2 (2014) 1767–1773.
[31] P. Mohammadi, M.M. Heravi, S. Sadjadi, Green synthesis of Ag NPs on magnetic polyallylamine decorated g-C_3N_4 by Heracleum persicum extract: efficient catalyst for reduction of dyes, Sci. Rep. 10 (2020) 6579–6588.
[32] P. Suchomel, L. Kvitek, R. Prucek, A. Panacek, A. Halder, S. Vajda, R. Zboril, Simple size-controlled synthesis of Au nanoparticles and their size-dependent catalytic activity, Sci. Rep. 8 (2018) 1–11.
[33] B.C. Choudhary, D. Paul, T. Gupta, S.R. Tetgure, V.J. Garole, A.U. Borse, D.J. Garole, Photocatalytic reduction of organic pollutant under visible light by green route synthesized gold nanoparticles, J. Environ. Sci. 55 (2017) 236–246.
[34] S. Vimalraj, T. Ashokkumar, S. Saravanan, Biogenic gold nanoparticles synthesis mediated by Mangifera indica seed aqueous extracts exhibits antibacterial, anticancer and anti-angiogenic properties, Biomed. Pharmacother. 105 (2018) 440–448.
[35] J. Panichikkal, R. Thomas, J.C. John, E.K. Radhakrishnan, Biogenic gold nanoparticle supplementation to plant beneficial *Pseudomonas monteilii* was found to enhance its plant probiotic effect, Curr. Microbiol. 76 (2019) 503–509.
[36] M.E. Khan, M.M. Khan, M.H. Cho, Environmentally sustainable biogenic fabrication of Au NP decorated-graphitic gC 3 N 4 nanostructures towards improved photoelectrochemical performances, RSC Adv. 8 (2018) 13898–13909.
[37] B. Dong, G. Liu, J. Zhou, A. Wang, J. Wang, R. Jin, H. Lv, Biogenic gold nanoparticles-reduced graphene oxide nanohybrid: synthesis, characterization and application in chemical and biological reduction of nitroaromatics, RSC Adv. 5 (2015) 97798–97806.
[38] A. Annamalai, V.L.P. Christina, D. Sudha, M. Kalpana, P.T.V. Lakshmi, Green synthesis, characterization and antimicrobial activity of Au NPs using Euphorbia hirta L. leaf extract, Colloids Surf. B 108 (2013) 60–65.
[39] H. Veisi, L. Mohammadi, S. Hemmati, T. Tamoradi, P. Mohammadi, In *Situ* immobilized silver nanoparticles on *Rubia tinctorum* extract-coated ultrasmall iron oxide nanoparticles: an efficient nanocatalyst with magnetic recyclability for synthesis of propargylamines by A^3 coupling reaction, ACS Omega 4 (2013) 13991–14003.
[40] H. Veisi, S.B. Moradi, P. Safarimehr, Silver nanoparticle-decorated on tannic acid-modified magnetite nanoparticles (Fe_3O_4@TA/Ag) for highly active catalytic reduction of 4-nitrophenol, Rhodamine B and methylene blue, Mater. Sci. Eng. C. 100 (2019) 445–452.
[41] H. Veisi, S. Azizi, P. Mohammadi, Green synthesis of the silver nanoparticles mediated by *Thymbra spicata* extract and its application as a heterogeneous and recyclable nanocatalyst for catalytic reduction of a variety of dyes in water, J. Clean. Prod. 170 (2018) 1536–1543.
[42] H. Veisi, T. Tamoradi, B. Karmakar, P. Mohammadi, S. Hemmati, In situ biogenic synthesis of Pd nanoparticles over reduced graphene oxide by using a plant extract (*Thymbra spicata*) and its catalytic evaluation towards cyanation of aryl halides, Mater. Sci. Eng. C 104 (2019) 109919–109927.
[43] H. Veisi, T. Ozturk, B. Karmakar, T. Tamoradi, S. Hemmati, In situ decorated palladium nanoparticles onto chitosan-encapsulated Fe_3O_4/SiO_2-NH_2 nanoparticles (Fe_3O_4/SiO_2-NH_2@CS/Pd NPs) as effective and recyclable catalyst in Suzuki-Miyaura coupling and 4-nitrophenol reduction, Carbohyd. Polym. 35 (2020) 115966–115973.
[44] T. Tamoradi, H. Veisi, B. Karmakar, Pd nanoparticle fabricated tetrahydroharman-3-carboxylic acid analog immobilized $CoFe_2O_4$ catalyzed fast and expedient C–C cross and C–S coupling, Chemistry Select 4 (2019) 10953–10959.
[45] B. Maleki, S. Hemmati, A. Sedrpoushan, S.S. Ashrafi, H. Veisi, Selective synthesis of sulfoxides and sulfones from sulfides using silica bromide as the heterogeneous promoter and hydrogen peroxide as the terminal oxidant, RSC Adv. (76) (2014) 40505–40510.
[46] H. Veisi, S. Razeghi, P. Mohammadi, S. Hemmati, Silver nanoparticles decorated on thiol-modified magnetite nanoparticles (Fe3O4/SiO2-Pr-S-Ag) as a recyclable nanocatalyst for degradation of organic dyes, Mater. Sci. Eng. C 97 (2019) 624–631.
[47] H. Veisi, S. Hemmati, P. Safarimehr, In *situ* immobilized palladium nanoparticles on surface of poly-methyldopa coated-magnetic nanoparticles (Fe_3O_4@PMDA/Pd): a magnetically recyclable nanocatalyst for cyanation of aryl halides with K_4[Fe(CN)$_6$], J. Catal. 365 (2018) 204–212.
[48] S. Mirfakhraei, M. Hekmati, F. Hosseini Eshbala, H. Veisi, Fe 3 O 4/PEG-SO 3 H as a heterogeneous and magnetically-recyclable nanocatalyst for the oxidation of sulfides to sulfones or sulfoxides, New J. Chem. 42 (2018) 1757–1761.
[49] B. Maleki, H. Veisi, Facile and efficient synthesis of bicyclic ortho-aminocarbonitrile derivatives using nanostructured diphosphate $Na_2CaP_2O_7$, Org. Prep. Proc. Int. 52 (2020) 232–237.
[50] H. Veisi, M. Ghorbani, S. Hemmati, Sonochemical *in situ* immobilization of Pd nanoparticles on green tea extract coated Fe_3O_4 nanoparticles: an efficient and magnetically recyclable nanocatalyst for synthesis of biphenyl compounds under ultrasound irradiations, Mater. Sci. Eng. C 98 (2019) 584–593.

[51] S.B. Chaleshtori, B. Shiran, M. Kohgard, H. Mommeni, A. Hafizi, M. Khodambashi, N. Mirakhorli, K. Sorkheh, Assessment of genetic diversity and structure of Imperial crown (*Fritillaria imperialis* L.) populations in the Zagros region of Iran using AFLP, ISSR and RAPD markers and implications for its conservation, Biochem. System Ecol. 42 (2012) 35–48.

[52] K. Kaneko, T. Katsuhara, Y. Kitamura, M. Nishizawa, Y.P. Chen, H.Y. Hsu, New steroidal alkaloids from the Chinese herb drug,"Bei-mu", Chem. Pharm. Bull 36 (1988) 4700–4705.

[53] C. Santhosh, V. Velmurugan, G. Jacob, S.K. Jeong, A.N. Grace, A. Bhatnagar, Role of nanomaterials in water treatment applications: a review, Chem. Eng. J. 306 (2016) 1116–1137.

[54] X. Lai, R. Guo, H. Xiao, J. Lan, S. Jiang, C. Cui, E. Ren, Rapid microwave-assisted biosynthesized silver/dandelion catalyst with superior catalytic performance for dyes degradation, J. Hazard. Mater. 371 (2019) 506–512.

[55] M.S. Najafinejad, P. Mohammadi, M. Mehdi Afsahi, H. Sheibani, Green synthesis of the Fe3O4@ polythiophen-Ag magnetic nanocatalyst using grapefruit peel extract: application of the catalyst for reduction of organic dyes in water, J. Mol. Liq. 262 (2018) 248–254.

[56] K. Naseem, Z.H. Farooqi, R. Begum, A. Irfan, Removal of Congo red dye from aqueous medium by its catalytic reduction using sodium borohydride in the presence of various inorganic nano-catalysts: a review, J. Clean. Prod. 187 (2018) 296–307.

[57] M. Atarod, M. Nasrollahzadeh, S.M. Sajadi, Green synthesis of Pd/RGO/Fe_3O_4 nanocomposite using *Withania coagulans* leaf extract and its application as magnetically separable and reusable catalyst for the reduction of 4-nitrophenol, J. Colloid Interface Sci. 465 (2016) 249–258.

[58] M. Nasrollahzadeh, E. Mehdipour, M. Maryami, Efficient catalytic reduction of nitroarenes and organic dyes in water by synthesized Ag/diatomite nanocomposite using *Alocasia macrorrhiza* leaf extract, J. Mater. Sci. Mater. Electron. 29 (2018) 10395–10410.

[59] S.H. Adyani, E. Soleimani, Green synthesis of Ag/Fe3O4/RGO nanocomposites by Punica Granatum peel extract: catalytic activity for reduction of organic pollutants, Int. J. Hydrog. Energy 44 (2019) 2711–2730.

[60] M.H. Salehi, M. Yousefi, M. Hekmati, E. Balali, Application of palladium nanoparticle-decorated *Artemisia abrotanum* extract-modified graphene oxide for highly active catalytic reduction of methylene blue, methyl orange and rhodamine B, Appl. Organometal. Chem. 33 (2019) 1.

[61] S. Sadjadi, P. Mohammadi, M. Heravi, Bio-assisted synthesized Pd nanoparticles supported on ionic liquid decorated magnetic halloysite: an efficient catalyst for degradation of dyes, Sci. Rep. 10 (2020) 6535.

[62] B.R. Ganapuram, M. Alle, R. Dadigala, A. Dasari, V. Maragoni, V. Guttena, Catalytic reduction of methylene blue and Congo red dyes using green synthesized gold nanoparticles capped by salmalia malabarica gum, Int. Nano Lett. 5 (2015) 215.

[63] W.S. Hummers, R.E. Offeman, Preparation of graphitic oxide, J. Am. Chem. Soc. 80 (1958) 1339.

[64] N. Esmaeili, P. Mohammadi, M. Abbaszadeh, H. Sheibani, Au nanoparticles decorated on magnetic nanocomposite (GO-Fe3O4/Dop/Au) as a recoverable catalyst for degradation of methylene blue and methyl orange in water, Int. J. Hydrog. Energ 44 (2019) 23002–23009.

[65] M. Kaloti, A. Kumar, Sustainable catalytic activity of Ag-coated chitosan-capped γ-Fe2O3 superparamagnetic binary nanohybrids (Ag-γ-Fe2O3@CS) for the reduction of environmentally hazardous dyes—a kinetic study of the operating mechanism analyzing methyl orange reduction, ACS omega 3 (2018) 1529–1545.

[66] K. Azad, P. Gajanan, Photodegradation of methyl orange in aqueous solution by the visible light active co:La:TiO_2 nanocomposite, J. Chem. Sci. 164 (2017).

[67] P. Deka, A. Hazarika, R.C. Deka, P. Bharali, Influence of CuO morphology on the enhanced catalytic degradation of methylene blue and methyl orange, RSC Adv. 6 (2016) 95292–95305.

[68] M. Dorraj, S. Sadjadi, M.M. Heravi, Pd on poly(1-vinylimidazole) decorated magnetic S-doped grafitic carbon nitride: an efficient catalyst for catalytic reduction of organic dyes, Sci. Rep. 10 (2020), 13440.